The formulator's guide to anti-oxygen inhibition additives

Branislav Husár, Samuel Clark Ligon [1], Harald Wutzel, Helmuth Hoffmann, Robert Liska [*,1]

Institute for Applied Synthetic Chemistry, Vienna University of Technology, Getreidemarkt 9/163, A-1060 Vienna, Austria

A B S T R A C T

Photo-curing has become increasingly popular in wood coating applications relative to thermally initiated processes due to increased curing rate with reduction in solvent and energy requirements. Stressing the last advantage, light emitting diodes (LEDs) utilize less energy and last longer than traditional Hg lamps and are commercially available now in wavelengths below 400 nm. Although photo-curing does have its advantages, an additional difficulty is encountered when this is performed in open-air since molecular oxygen inhibits radical polymerization. This leads to insufficiently cured films that remain tacky at the surface. Although nitrogen gas inerting can be highly successful in excluding oxygen, chemical additives are often preferable to the small and medium-sized enterprise (SME) end user. A variety of additives have been introduced over the last 30 years both in the scientific and patent literature. We have chosen to experimentally reinvestigate the applicability of some of these additives (hydrogen donors, functional monomers, reducing agents, CO_2 producing agents, and singlet oxygen scavengers), applying them to a urethane acrylate base formulation. Curing was performed with LED irradiation and effectiveness assessed by FTIR in transmission mode.

© 2014 Elsevier B.V. All rights reserved.

1. Introduction

UV curable coatings are an increasingly popular alternative to traditional solvent-borne coatings and already constitute 11% of the European wood coatings market [1]. As UV curing requires less energy than thermal curing and avoids the release of volatile organic compounds (VOCs), the market share of UV based coatings is predicted to continue to grow [2]. Regardless of the application, UV based coatings are based by and large on the radical polymerization of acrylates. This chemistry is fast and versatile but has one serious and still today unresolved flaw. That problem is the inhibition of radical polymerization by ground state molecular oxygen causing incomplete curing and leading generally to diminished mechanical performance and tacky surfaces [3–5]. In the coatings industry, this problem has been traditionally mitigated by using a combination of two photoinitiators, whose absorption characteristics match the emission bands of the mercury lamp [6]. Good through cure is achieved using a photoinitiator absorbing light at 365 and 405 nm (e.g. mono- or bis-acyl phosphine oxide). To compensate for oxygen inhibition, which is particularly acute at the surface of the coating, a lower wavelength ($\lambda < 350$ nm) photoinitiator (e.g. α-hydroxy acetophenone) is additionally used.

Light emission diodes (LEDs) are 60–80% more energy efficient than conventional UV lamps and are commercially available in wavelengths down to 365 nm. In addition, LEDs do not contain mercury, do not produce ozone, do not require a warm-up phase, and provide a longer lasting and more constant output. For these reasons the use of UV-LED curable coatings is predicted to expand remarkably although technical challenges still remain [7]. LEDs emit essentially monochromatic light, which means that curing is only effective when there is good overlap with the absorbance of the utilized photoinitiator. Since commercially available LEDs with high effective irradiance do not emit below 365 nm, traditional formulations based on lower wavelength photoinitiators will not be effective. This is not a major problem though since there are a number of commercial photoinitiators that do absorb at and beyond 365 nm.

To overcome the associated problems of oxygen inhibition, manufacturers are often reliant on rather costly gas inerting, typically with nitrogen or alternatively with carbon dioxide [8,9]. Higher costs for additional equipment and nitrogen supply might be partially compensated by faster curing and reduced photoinitiator loading [10,11]. Utilization of wax additives [12], liquid barriers, or lamination are other options but all require additional process
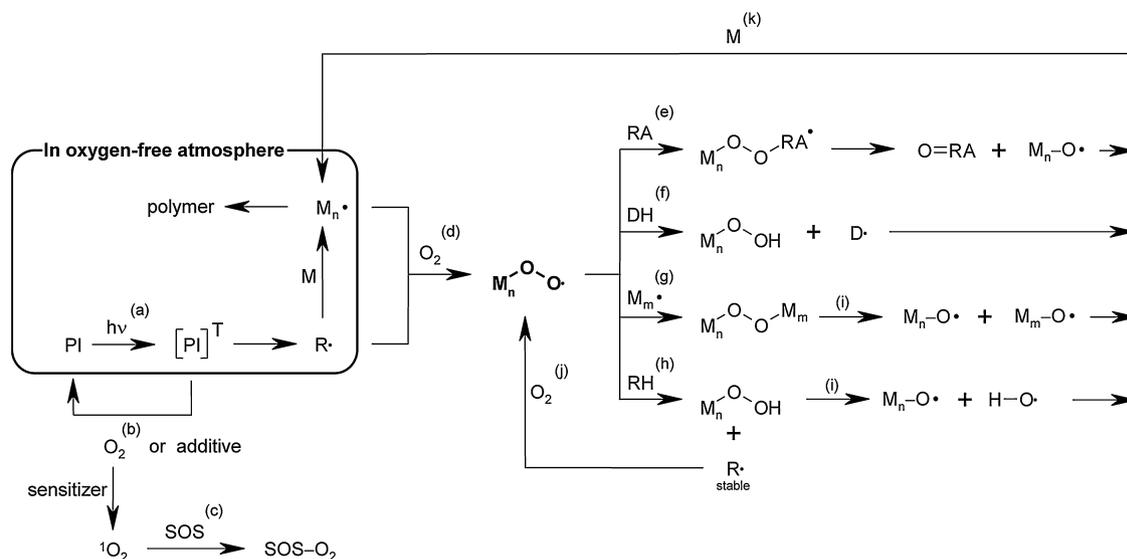
Scheme 1. Mechanistic explanation of oxygen inhibition and strategies to mitigate it: (a) initiation stage strategies (i.e., inerting, lamination, light source, molecular inerting, and photoinitiators), (b) quenching of excited state of photoinitiator, (c) singlet oxygen scavengers, (d) formation of unreactive peroxyl radicals from initiating or propagating radical, (e) reducing agents, (f) hydrogen donors, (g) termination by radical–radical recombination, (h) hydrogen abstraction, (i) peroxide decomposition, (j) scavenging of a molecule of oxygen, and (k) reinitiation of polymerization.

steps making them inappropriate for the small and medium-sized enterprise (SME) end users of low-cost wood coatings. Yet another way to reduce oxygen inhibition is to increase the effective irradiance of the curing light, and in fact today's commercial LED modules provide output comparable to Hg lamps [13]. This option is limited to a certain threshold, above which termination overtakes propagation.

While the aforementioned physical methods for dealing with oxygen inhibition can be successful, they tend be less appropriate for the intended user of the coating. Fortunately, a multitude of chemical additives have been developed over the years. The additive is typically used at a concentration less than 5% of the total formulation or alternatively modification is made to the actual monomers in the formulation [3].

Anti-oxygen inhibition strategies can be classified according to the role or roles they play on the reactions of photoinitiation, radical polymerization, and associated side reactions with oxygen (Scheme 1). Photoinitiators (PI) are the first class of additives to be considered where effectiveness is based on absorption, radical generation ($R^\bullet$), and transformation of monomer (M) into a propagating radical ($M_n^\bullet$). When this reaction occurs in the presence of oxygen, however, the tendency is to give the rather unreactive peroxyl radical ($M_nOO^\bullet$) in a competing reaction. Formation of $M_nOO^\bullet$ can be minimized by reducing the concentration of oxygen during or prior to initiation. This can be achieved e.g. by addition of sensitizers in combination with reactive dienes that trap singlet oxygen [14–16] or by using molecules, which photodecompose to generate CO_2 or N_2 to lower local oxygen concentration (e.g. *N*-phenyl glycine or oxime esters) [17].

If oxygen is not completely removed prior to initiation, all is not lost. Hydrogen donors, for instance, can react with $M_nOO^\bullet$ to form M_nOOH and a new reactive radical ($D^\bullet$) capable of propagating polymerization or alternately scavenging an additional molecule of oxygen. Typical hydrogen donors are amines [18], thiols [19], and ethers [20] but also less common silanes [21], stannanes [22], hydrogen phosphites [23], or aldehydes [24]. Unreactive peroxyl radicals $M_nOO^\bullet$ can also be transformed by reducing agents to a new reactive radical ($M_nO^\bullet$) that may propagate polymerization. Typical representatives of this group of reagents are phosphines [25], phosphites [26], boranes (which are often complexed with amines to improve stability) [27], and also certain metal complexes

[28]. Finally, strategies to regenerate radicals by decomposing peroxide compounds (M_nOOM_m and M_nOOH) with photosensitizers are considered [29].

Strategies based on modification to the monomer formulation may not be accurately depicted by Scheme 1 explaining the role of additives. Such strategies include acrylates bearing aforementioned reactive functional groups [20], multifunctional acrylates [30], acrylated dendrimers [31], *N*-vinyl amides [32], donor/acceptor type monomers [33], and hybrid radical/cationic systems [34].

Due to the enormous importance of photopolymerization in industry, hundreds of scientific papers and patents on strategies to overcome oxygen inhibition have been published and recently reviewed [3–5]. Unfortunately, individual anti-oxygen inhibition additives have tended to be studied under different conditions (using different monomers, different additive concentrations, different initiators, different film thicknesses and different light sources run at different intensities for different exposure times) and then evaluated using different criteria (IR, pendulum hardness, solvent rubs, etc.), which makes it impossible to quantitatively compare these additives. In this work, we have attempted to assess the effectiveness of various anti-oxygen inhibition additives under the same conditions. We utilize the same base urethane acrylate formulation and give to this a consistent concentration of additive and cure with LED irradiation of equal effective irradiance and exposure. Film thickness and effective irradiance were both held intentionally low, which exacerbate the problem of oxygen inhibition and made the effectiveness of any particular additive easier to assess. Moreover, a type I photoinitiator with a long triplet state lifetime is more likely to be affected by quenching by oxygen and the additives. To reduce subjectivity in data analysis, a Visual Basic for Applications (VBA) based macro was created that calculates double bond conversion (DBC) from integrated IR spectral bands based on Gaussian peak deconvolution.

2. Material and methods

2.1. Chemicals

Aliphatic difunctional polyether urethane acrylate (BR-344; Bomar), alkyl (C_{12}–C_{15}) bisphenol A phosphite (D613; Dover),
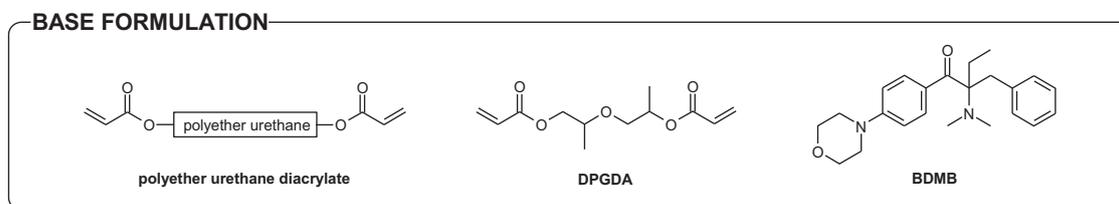
Fig. 1. Components of the base formulation.

4-anisaldehyde (PAA; 98%, Aldrich), 2-benzyl-2-(dimethylamino)-4′-morpholinobutyrophenone (BDMB; Lambson), 3,9-bis(octadecyloxy)-2,4,8,10-tetraoxa-3,9-diphosphaspiro[5.5]undecane (BOTDBU; Sigma–Aldrich), n-butyl acetate (98%, Merck), n-butyl acrylate (BASF), dimethylamine–borane complex (Me₂NH·BH₃; 97%, Aldrich), dioleyl hydrogen phosphite (D253; Dover), 2,5-diphenyl furan (DPF; 98%, Alfa Aesar), dipropylene glycol diacrylate (DPGDA; Isovolta), ethylene sulphite (ETS; 99%, Fluka), N-methyl pyrrolidone (NMP; Merck), isopropyl thioxanthone (ITX; Lambson), pentaerythritol tetrakis(3-mercaptopropionate) (PETMP; Bruno Bock), N-phenyl glycine (NPG; 93%, Acros), 1-phenyl-1,2-propanedione-2-(O-ethoxycarboxy)oxime (PDO; Lambson), phenylthioacetic acid (PTAA; 96%, Aldrich), poly(dipropyleneglycol) phenyl phosphite (D12; Dover), tetraphenyl dipropyleneglycol diphosphite (D11; Dover), tribenzyl amine (Bz₃N; 99%, Fluka), tri-n-butyl stannane (Bu₃SnH; 97%, Aldrich), trimethylolpropane tris(3-mercaptopropionate) (TMPMP; Bruno Bock), trioctyl phosphine (TOP; 90%, Fluka), triphenyl phosphine (PPh₃; 95%, Sigma–Aldrich), triphenyl phosphite (P(OPh)₃; 97%, Fluka), tris(tridecyl) phosphite (D49; Dover), tris(trimethyl silyl) silane (TTMSS; 97%, ABCR), and N-vinyl pyrrolidone (NVP; 98%, Merck) were used as received. 1,4-Diazabicyclo[2.2.2]octane (DABCO) was recrystallized from ethyl acetate before use. N-methyl diethanolamine (MDEA) was redistilled before use. 9,10-Dibutyl anthracene (DBA) [14], N-methyl-N-phenyl glycine (NMNPG) [35], and O-benzoyloxime benzaldehyde (POE) [36] were synthesized according to previously reported methods.

2.2. Sample preparation

The base formulation (Fig. 1) represents a simplified UV-curable woodcoating. It consisted of a 1:1 mixture (weight) of polyether urethane diacrylate and DPGDA with 2 wt% of BDMB as a photoinitiator. Various additives (Fig. 2) were then added to this base formulation in amounts expressed in molar equivalents to BDMB. Films with uniform layer thickness (6 μm) were prepared by applying the formulation on a roughened polyethylene foil with the help of a wire-wound rod no. 8 (UV process supply). If not stated otherwise, the formulation was always freshly prepared. Low layer thickness exacerbates the problem of oxygen inhibition and provides an optimal IR absorbance for the reference carbonyl peak ($A \approx 0.7$).

2.3. LED Irradiation

Freshly prepared films on polyethylene foil were held within a sample cell with rubber gaskets and placed into the FTIR instrument (Bruker V80). The cover of the spectrometer sample chamber was fitted with a custom-built cover plate with three separate CAD-CAM printed holder pieces. Into one of these holders was placed a 365 nm LED and into another a 400 nm LED (both powered by an external OmniCure LX400 power source). Position of both lamps was approximately 20 mm from the sample cell with an angle of incidence of approximately 50° (see Supplementary data). Sample films without ITX were irradiated directly within the FTIR spectrometer for 10 s using the 365 nm LED lamp. The LED was pre-calibrated to provide effective irradiance of 120 mW cm⁻² at the surface of the film as determined by an Ocean Optics USB 2000+ Spectrometer. For samples prepared with ITX, the film was irradiated for 10 s simultaneously with two LED lamps (365 and 400 nm with each set to give effective irradiance of 60 mW cm⁻² at the surface of the film). Curing for all samples rapidly reached an asymptote (as monitored by real time IR) and was found to be essentially complete within 10 s. Following irradiation, the FTIR spectra of the cured films were measured using the same settings as before. All measurements were performed with at least 5 different samples for each formulation to ensure the reproducibility of the results.

2.4. Determination of double bond conversion

The consumption of acrylate double bonds was monitored by the decrease of the peaks at 1620 and 1637 cm⁻¹. The peak at 1620 cm⁻¹ is slightly overlapped by the peak at 1600 cm⁻¹. The peaks at 810 and 1450 cm⁻¹ were not used due to strong overlap by adjacent peaks that could not be resolved by peak deconvolution. DBC values were determined using a custom built Microsoft Excel VBA macro (see Supplementary data) in order to accelerate the calculations and to reduce user bias. IR data files in all cases were collected from 2000 cm⁻¹ to 1500 cm⁻¹ with scan resolution of 4 cm⁻¹ and exported in *.dpt format. The macro performed the following steps with every recorded IR spectrum:

(1) Baseline correction by subtraction of a straight line defined by two points (local minimum from 1570 to 1580 cm⁻¹ and a point at 1850 cm⁻¹ set to the average y-value from 1850 to 2000 cm⁻¹).
(2) Calculates Gaussian curves to the peaks at 1600, 1620, and 1637 cm⁻¹ and adjusts height and width terms to minimize the value between the sum of the curves and the spectrum data.
(3) Integration by rectangular summation of the carbonyl band at 1726 cm⁻¹.
(4) DBC is finally calculated using Eq. (1), where A_{0s} and A_{10s} are corresponding peak areas of uncured and cured sample respectively. Eq. (2) is used for the ITX-containing samples due to the overlap with the carbonyl band of ITX. DBC values calculated from Eq. (2) are slightly higher than from Eq. (1).

$$\text{DBC} = \left(1 - \frac{A_{10\,s}(1620\,\text{cm}^{-1}) + A_{10\,s}(1637\,\text{cm}^{-1})}{A_{0s}(1620\,\text{cm}^{-1}) + A_{0s}(1637\,\text{cm}^{-1})} \times \frac{A_{0s}(1726\,\text{cm}^{-1})}{A_{10\,s}(1726\,\text{cm}^{-1})}\right) \times 100\% \quad (1)$$

$$\text{DBC} = \left(1 - \frac{A_{10\,s}(1620\,\text{cm}^{-1})}{A_{0s}(1620\,\text{cm}^{-1})} \times \frac{A_{0s}(1726\,\text{cm}^{-1})}{A_{10\,s}(1726\,\text{cm}^{-1})}\right) \times 100\% \quad (2)$$
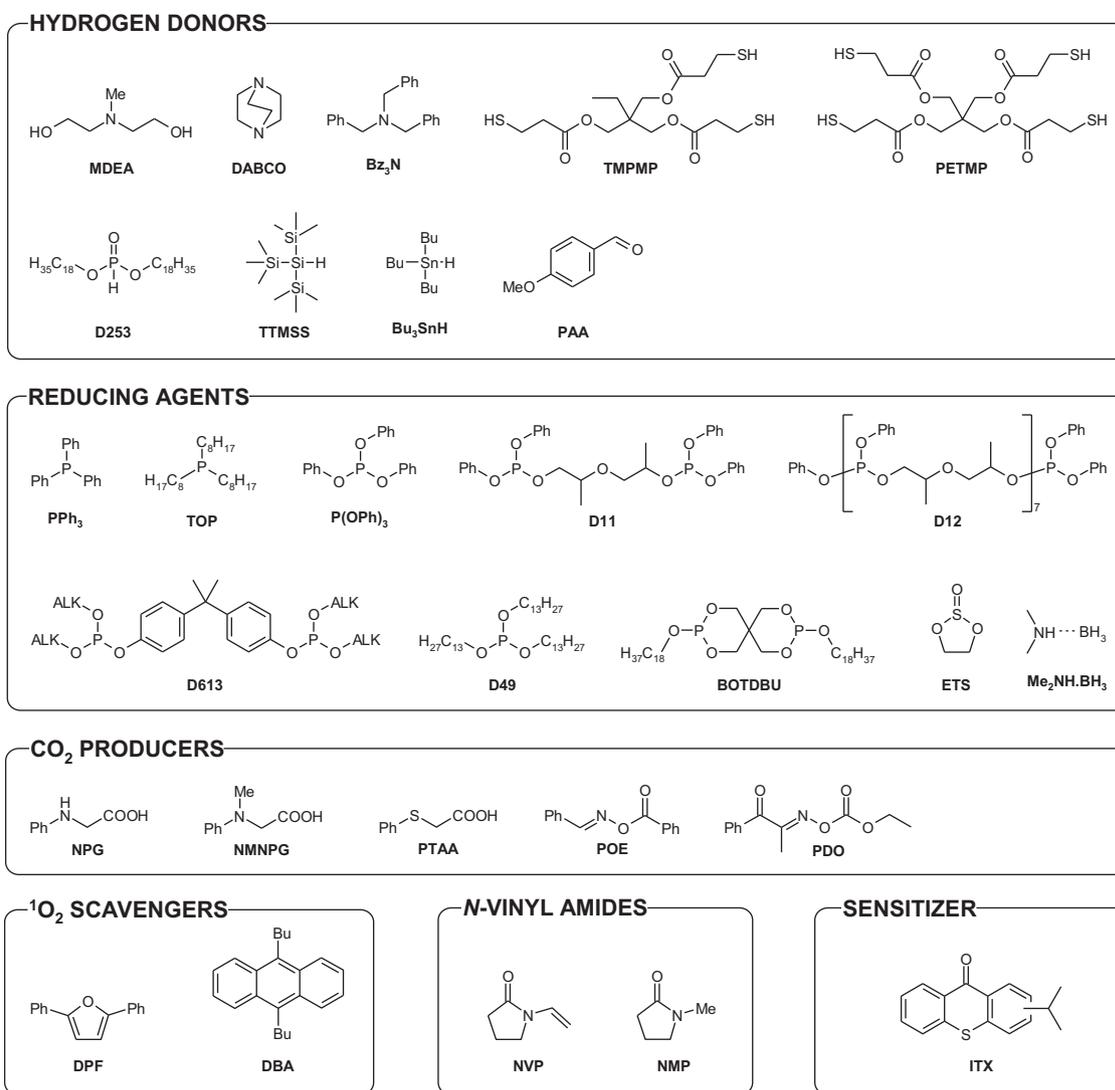
Fig. 2. Chemical structures of the tested additives.
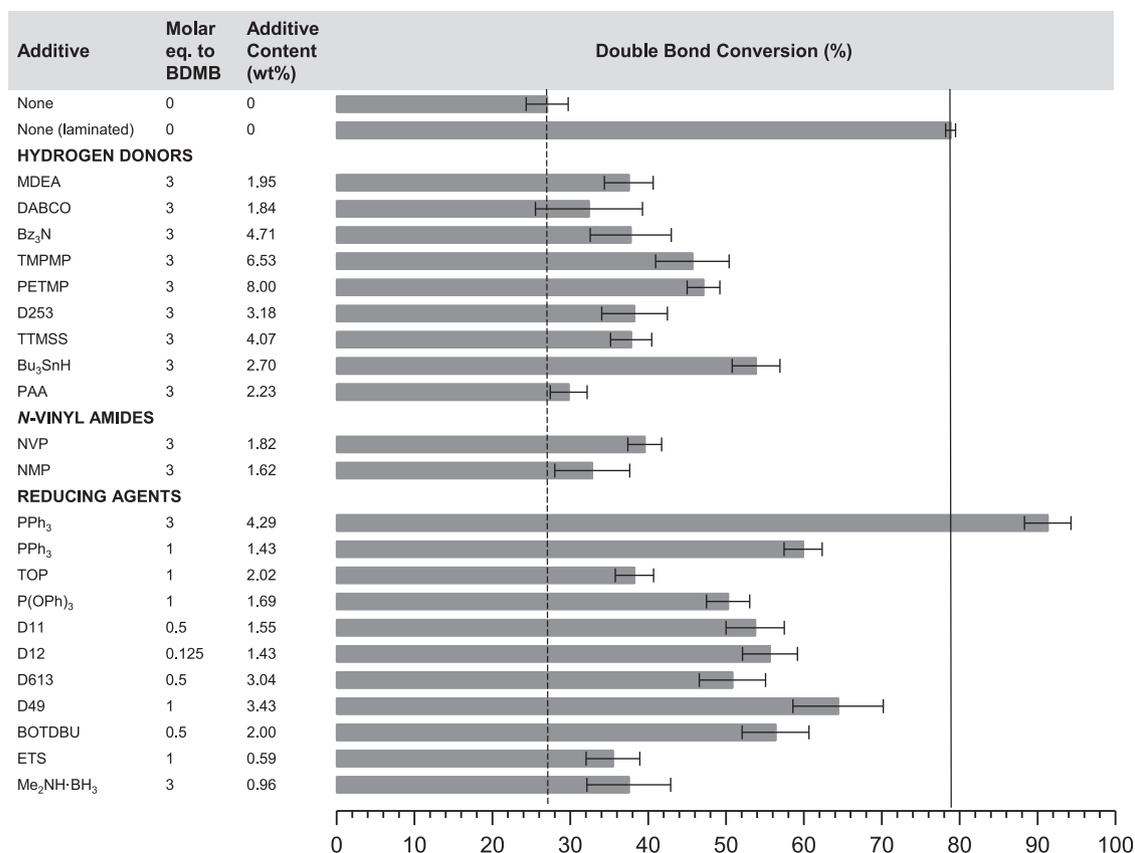
3. Results and discussion

In this study, the effectiveness of different additives in mitigating oxygen inhibition is assessed by monitoring the DBC of the cured additive containing formulation and comparing to the DBC of the cured base (additive-free) formulation. FTIR is a precise and quantitative method for assessing cure performance, but it is limited at high conversions where DBC may not correlate well with the mechanical properties of the cured coating [37]. By using low effective irradiance and thin films we exacerbated the problem of oxygen inhibition and made the effectiveness of individual additives easier to gauge. It should thus be noted that the ability of an additive to improve DBC does not guarantee that it will also improve hardness, since some additives can also act as plasticizers.

Typical UV-curable wood coating formulations consist of an acrylated oligomer, reactive diluent, filler, initiator(s), and may also contain a low amount of dispersing and anti-foaming agents. To avoid possible interaction with extra additives, we chose a simplified base formulation consisting of a polyether urethane diacrylate, a reactive diluent (DPGDA), and a photoinitiator (BDMB). It should be noted that oxygen inhibition is already mitigated to some extent by this formulation since both monomers used (oligomer and DPGDA) have oligoether backbones and thus contain abstractable hydrogen atoms. One could expect an even more pronounced effect
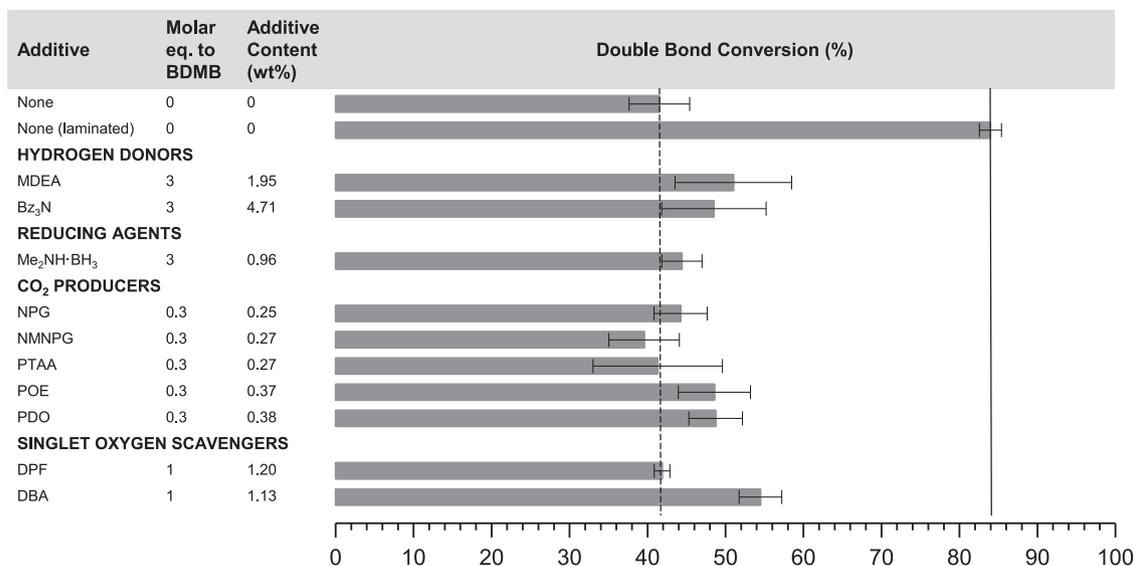
in open-air curing of other monomers lacking abstractable hydrogen. The chosen base formulation had to fulfill two important criteria: first, a sufficiently high viscosity ($\approx 1\,\mathrm{Pa\,s}$) was required to prevent unwanted flow of the vertical sample film during IR spectroscopy. Second, it was important that the acrylate CH=CH$_2$ stretching bands (1620 and 1637 cm^{-1}) did not overlap strongly with the signals of other components in the mixture.

To this base formulation, anti-oxygen inhibition additives were added in amounts expressed in molar equivalents to BDMB. The amount of the standard amine MDEA was set to 2 wt% that corresponds to 3 eq. All other hydrogen donors and *N*-vinyl amides were used in 3 eq. too. Reducing agents and singlet oxygen scavengers are generally heavier molecules and were used in 1 eq. For instance, 1 eq. of a typical reducing agent P(OPh)$_3$ corresponds to 1.7 wt% that is almost 2 wt% as in the case of MDEA. Phosphites with 2 phosphorus atoms (D11, D613, and BOTDBU) and 8 phosphorus atoms (D12) were used in 0.5 eq. and 0.125 eq. respectively. Sensitizer (ITX) was used in 0.1 eq. since it is yellow and does not photobleach. Thus only low amounts are acceptable for clear coat applications. CO$_2$ producers were used in 0.3 eq. because they react equimolarly with ITX. More details on the reaction mechanisms of all additives are given in a recent review paper [3].

The results are summarized in Figs. 3 and 4. Fig. 3 shows the results acquired after curing at 365 nm in air with 2 wt% of BDMB

| Additive	Molar eq. to BDMB	Additive Content (wt%)	Double Bond Conversion (%)
None	0	0	
None (laminated)	0	0	
HYDROGEN DONORS			
MDEA	3	1.95	
DABCO	3	1.84	
Bz₃N	3	4.71	
TMPMP	3	6.53	
PETMP	3	8.00	
D253	3	3.18	
TTMSS	3	4.07	
Bu₃SnH	3	2.70	
PAA	3	2.23	
***N*-VINYL AMIDES**			
NVP	3	1.82	
NMP	3	1.62	
REDUCING AGENTS			
PPh₃	3	4.29	
PPh₃	1	1.43	
TOP	1	2.02	
P(OPh)₃	1	1.69	
D11	0.5	1.55	
D12	0.125	1.43	
D613	0.5	3.04	
D49	1	3.43	
BOTDBU	0.5	2.00	
ETS	1	0.59	
Me₂NH·BH₃	3	0.96	

Fig. 3. Double bond conversions of formulations containing 2 wt% of BDMB as photoinitiator and various additives cured at 365 nm. Note that phosphite concentration is based on concentration of P-atoms (thus 0.5 eq. for molecules with 2 P-atoms and 0.125 eq. for molecules with 8 P-atoms).

| Additive	Molar eq. to BDMB	Additive Content (wt%)	Double Bond Conversion (%)
None	0	0	
None (laminated)	0	0	
HYDROGEN DONORS			
MDEA	3	1.95	
Bz₃N	3	4.71	
REDUCING AGENTS			
Me₂NH·BH₃	3	0.96	
CO₂ PRODUCERS			
NPG	0.3	0.25	
NMNPG	0.3	0.27	
PTAA	0.3	0.27	
POE	0.3	0.37	
PDO	0.3	0.38	
SINGLET OXYGEN SCAVENGERS			
DPF	1	1.20	
DBA	1	1.13	

Fig. 4. Double bond conversions of formulations containing 2 wt% of BDMB as photoinitiator, 0.14 wt% of ITX as sensitizer, and various additives cured simultaneously at 365/400 nm.

as a photoinitiator. The dashed line displays the DBC (27%) achieved from the curing of the base formulation under air without any additive. The full line displays the DBC (79%) obtained from the same base formulation cured under laminated conditions between two polyethylene foils. Since no efforts were made to remove dissolved oxygen by pre-purging, the maximum attainable DBC value for this formulation is likely even higher.

Data presented in Fig. 4 were acquired after dual-wavelength curing at 365/400 nm in air. All of these samples contain 2 wt% of BDMB (which absorbs at 365 nm) as photoinitiator and 0.14 wt% of ITX (which absorbs at 400 nm) as additional sensitizer. Dual wavelength curing might be advantageous as it can trigger two different initiating processes simultaneously. As a testament to success, the addition of ITX in an amount as small as 0.14 wt% improves DBC
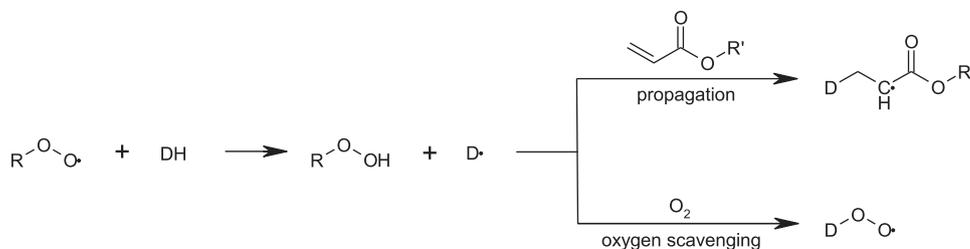
Scheme 2. Radical reinitiation via hydrogen donation.
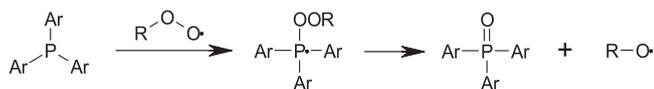
Scheme 3. Radical reinitiation via phosphine oxidation.

of the base formulation from 27% (365 nm, 120 mW cm^{-2}) to 42% (365/400 nm, 60 + 60 mW cm^{-2}) at the same total effective irradiance and exposure. The dashed line displays the DBC (42%) achieved when curing the base formulation with ITX under air using both lamps. The full line shows the DBC (84%) of this formulation cured under laminated conditions.

3.1. Hydrogen donors

The ability for hydrogen donors to mitigate oxygen inhibition was first described in Type II photoinitiation systems, and was later discovered to be effective for Type I photoinitiation [6]. A general scheme for the mechanism of hydrogen donation is shown in Scheme 2. The hydrogen donor provides a hydrogen atom, which caps the already formed peroxyl radical. The peroxyl radical does not have sufficient propagating activity to react with an acrylate, however the newly formed donor radical (D•) can reinitiate polymerization or scavenge a molecule of oxygen. The schematic does not indicate the nature of the hydrogen donor and indeed this can have an impact on performance.

Amines have been commonly used as coinitiators for decades with tertiary amines being preferred due to lower volatility and higher reactivity. Donation of hydrogen by a carbon adjacent to nitrogen provides an alkyl radical stabilized in an anti-coplanar arrangement with the lone pair orbital on nitrogen permitting sharing of π-electrons. In our experiments using a single 365 nm LED, N-methyl diethanolamine (MDEA) was found more effective than 1,4-diazabicyclo[2.2.2]octane (DABCO), which could be due to ring strain hindering the above mentioned resonance. Addition of MDEA to the formulation increased the DBC from 27% to 38%, while with DABCO only 32% DBC was reached. An even higher DBC value was expected for tribenzyl amine (Bz$_3$N), which should lead to a better stabilized alkyl radical due to additional resonance stabilization from the phenyl group. Bz$_3$N provided however a DBC value essentially the same as that of MDEA. In the end, MDEA is preferred since Bz$_3$N is a solid and has a much higher molecular weight, which means twice the mass is required to provide the same effect. For the dual wavelength experiments, MDEA gives similar enhancement in the presence of a small amount of ITX with DBC increasing from 42% to 51%. In this system, initiation can occur directly with BDMB which absorbs at 365 nm or via Type II initiation where ITX acts as sensitizer and MDEA as both coinitiator and as an anti-oxygen inhibition additive. Bz$_3$N by comparison seems to be less effective in the presence of ITX although it should be noted that the standard deviation for the IR measurements was relatively high. While MDEA provides noticeable improvement in open-air photocuring, the formulator should be advised that odor, volatility, water solubility, and reactivity with atmospheric acids are issues with low

molecular amines. For these reasons, amine acrylate monomers are a good alternative.

Thiols are effective hydrogen donors and oxygen scavengers. In this study, a trithiol (TMPMP) and a tetrathiol (PETMP) were used at concentrations of 6.5 and 8 wt% respectively using the 365 nm LED light source (Fig. 3). Although these are relatively high weight percentages for additives, these multifunctional thiols copolymerize in a chain transfer mechanism with acrylates and therefore do not leach from the final coating. In comparison to amines tested at equal molar concentrations, TMPMP and PETMP provided superior results (46% and 47% DBC respectively). The main problems associated with thiols are their bad odor and their low storage stability although attempts have been made to overcome these drawbacks. The problem of odor can be overcome by using polymeric thiols that lack cleavable ester groups and storage stability can be significantly improved with use of appropriate radical inhibitors and phosphonic acid coadditives [38,39]. The universality of these solutions is yet to be determined.

Hydrogen phosphites HP(O)(OR)$_2$ have been scarcely reported as anti-oxygen inhibition additives [23]. In principal, one molecule of hydrogen phosphite is capable of reducing two peroxyl radicals: after reducing a peroxyl radical by donation of a hydrogen atom, the formed phosphorous radical can reduce another peroxyl radical to form a reactive alkoxyl radical. In this study, dioleyl hydrogen phosphite (D253) was tested. It provides an enhancement in cure comparable to MDEA (38% DBC). Hydrogen phosphites thus do not seem to have any advantage over amines.

Silanes were previously reported to be very effective hydrogen donors [22]. Tris(trimethylsilyl)silane (TTMSS) was chosen due to the fact that it has the lowest Si—H bond energy and donates a hydrogen atom the fastest out of previously tested silanes. In comparison, the Si—H bond energy in TTMSS (79.8 kcal mol^{-1}) [22] is considerably lower than the C—H bond energy in MDEA (87.1 kcal mol^{-1}) [40]. Moreover, the formed silyl radical after scavenging a molecule of oxygen forms a peroxyl radical (SiOO•) that may rearrange to provide a new reactive silyl radical that may then react with monomer or an additional molecule of oxygen [21]. Despite these findings, under our experimental conditions TTMSS gives a comparable improvement to MDEA using the same molar amount. Since TTMSS is air and water sensitive, heavier, and more expensive, amines seem to be the better option.

Tri-n-butyl stannane (Bu$_3$SnH) is obviously not of industrial interest due to high toxicity and high moisture sensitivity. Nevertheless, it was tested since it was reported as one of the most effective hydrogen donors. The Sn—H bond energy in Bu$_3$SnH molecule is only 73.8 kcal mol^{-1} and hydrogen atom donation to peroxyl radical is about 10 times faster than in the case of TTMSS [22]. Despite partial hydrolysis of Bu$_3$SnH in non-dried base formulation, the curing reached as much as 54% DBC.

Aldehydes have been described as effective coinitiators in Type II initiating systems [24]. In this study, aldehydes were tested as hydrogen donors in the presence of a Type I initiator. 4-Anisaldehyde (PAA) was selected since the *para*-methoxy should help stabilize the benzoyl radical formed after hydrogen
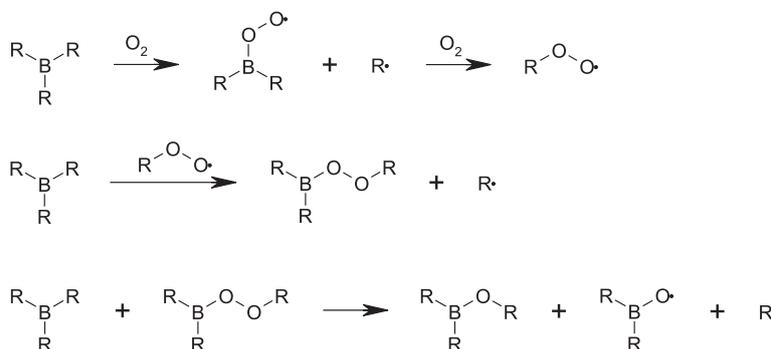
Scheme 4. Radical reactions of alkyl boranes and oxygen species.

abstraction. However, addition of PAA provided only a negligible improvement within the error of the measurement.

3.2. N-vinyl amides

N-vinyl pyrrolidone (NVP) has often been added to UV curable resins to reduce viscosity and improve the curing in air. A major advantage of this compound is that it copolymerizes with acrylates and remains as part of the cured formulation. Its mechanism of action is not completely understood although three hypotheses exist: (*i*) NVP acts as an oxygen scavenger similar to amines or (*ii*) NVP forms an exciplex with oxygen to produce reactive radicals or (*iii*) NVP forms a donor–acceptor complex with acrylate [32].

Here we compare NVP with its non-vinyl analog N-methyl pyrrolidone (NMP). It is known from the literature that both give better cure although NVP is more effective [32]. These results were confirmed in this study: NVP gives 40% DBC while NMP gives just 33% DBC after curing in air (365 nm LED lamp). Although NVP seems to be an effective additive, similar results can be obtained with low molecular weight additives of similar molecular weight. For instance, butyl acrylate gives 36% DBC and butyl acetate gives 34% DBC under the same curing conditions. It is known that dilution of multifunctional monomers with monofunctional monomers leads to increase of DBC due to increased mobility of monomers. One must be also aware of increased hydrophilicity of the cured photopolymer, which is generally undesirable in wood coating applications.

3.3. Reducing agents

Phosphines and phosphites are both known to be very effective antioxidants. In photopolymerization, they may be oxidized by peroxyl radicals. In the process, new radicals are formed that may propagate reaction (Scheme 3).

As Fig. 3 illustrates, triphenyl phosphine (PPh₃) is one of the most effective additives in this study. Under the testing conditions, 3 eq. gives a curing performance beyond that of the laminated sample (91% DBC) with no final surface tack. Despite its outstanding performance, PPh₃ suffered from very poor storage stability in our coating formulations: DBC in cured films from aged formulations dropped from 91% to 71% after 1 day of storage and to 67% after 7 days upon storage in air. After a week, the formulation became more viscous and some precipitate appeared as well. It is more realistic to use only 1 eq. instead of 3 eq. A freshly prepared formulation containing 1 eq. of PPh₃ gives 60% DBC, which decreased to 52% after 4 weeks of storage at room temperature in a sealed flask under air. This formulation also became slightly turbid and more viscous. Moreover, the concentration of C=C double bonds in the formulation was decreased by 10% upon storage although the formulation did not gel. Based on its high potential for reducing oxygen inhibition, a method for improving the storage stability of PPh₃

would be desirable. An aliphatic trioctyl phosphine (TOP) was also tested but proved to be much less effective than PPh₃. DBC reached only 38%. Moreover, alkyl phosphines are known to be oxidized more readily by molecular oxygen in comparison to PPh₃ [41].

Phosphites proved to be the second most effective type of additive. Six different phosphite additives (P(OPh)₃, D11, D12, D613, D49, and BOTDBU) were tested and gave impressive results ranging from 50 to 64% DBC. Among the different phosphites, the aromatic triphenyl phosphite (P(OPh)₃) was the least effective (50% DBC) that can be attributed to the reaction with alkoxyl radicals to form phenoxyl radicals, which act as radical inhibitors. On the other hand, the aliphatic tris(tridecyl) phosphite (D49) gave the highest DBC in this study (64%), exceeding even PPh₃. Hybrid aromatic/aliphatic phosphites provided DBC values between 51 and 56%. Phosphites are generally liquids and easy to dissolve in the formulation. Only BOTDBU is a solid and rapidly precipitates from the formulation. In addition to improving cure performance, utilization of these additives is quite realistic since they are already industrially used as stabilizers for PVC processing. Importantly, price, viscosity, and color appear to be sufficiently low for wood coating applications. However, phosphites exhibit storage stability problems in some ways comparable to PPh₃. A slightly higher viscosity and turbidity was observed upon storage in a sealed flask under air for 4 weeks. In the case of the oligomeric D12, the DBC dropped from 56% to 44% after 4 weeks of storage. It is worth noting that phosphites also have a distinct phenolic odor independent of molecular weight, which could be detected even in the least volatile oligomeric D12. A recent patent from Eastman Kodak describes the complexing of phosphites with aldehydes, which is claimed to reduce the odor and to improve the storage stability [42].

Sulfites are popular antioxidants in food and color preservation but are not traditionally used in photocurable resins. As a representative of this class of molecules, we chose ethylene sulfite (ETS). Both phosphines and phosphites easily outperform ETS, which gives only 36% DBC. Based on these results, the mediocre performance and irritancy make them less appealing for industrial application.

Boron based reducing agents are commonly used in thermal initiating systems; however the use of boranes in photocurable formulations is not so well established. An interesting feature of boranes is that in the presence of oxygen they can act as radical initiators (Scheme 4). Although it may at first sound like a simple solution to overcome oxygen inhibition, the main problem in this case is that formulations are not stable and react prematurely. A useful strategy for stabilizing boranes during storage and yet to keep them available for intended oxygen inhibition is to complex them with an amine [27]. Borane–amine complexes have previously been used as coinitiators with a Type II photoinitiator. Hydrogen abstraction from the amine releases borane (BH₃), which provides reactive radicals after the reaction with dissolved oxygen. We attempted to use the dimethylamine–borane complex
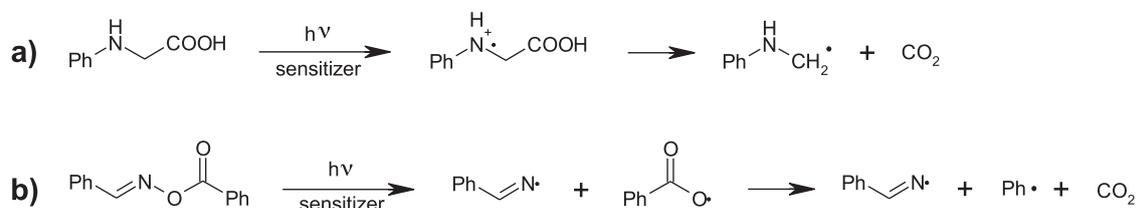
Scheme 5. Photo-induced gas generation from (a) *N*-phenyl glycine (NPG) and (b) *O*-benzoyloxime benzaldehyde (POE).
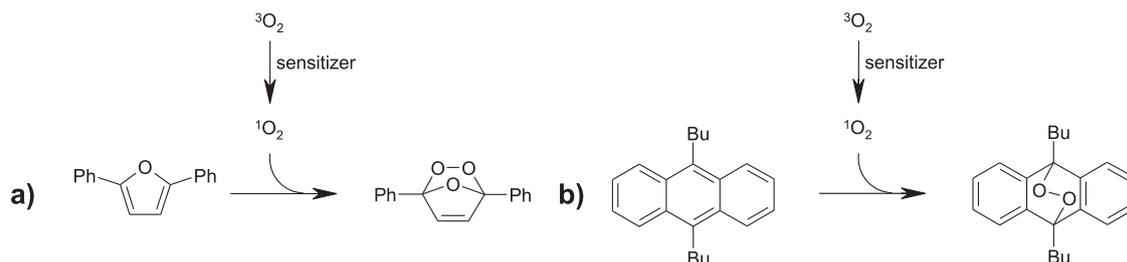
Scheme 6. Singlet oxygen scavenging via [4 + 2] cycloaddition with (a) diphenyl furan (DPF) and (b) dibutyl anthracene (DBA).

Table 1
The formulator's guide to anti-oxygen inhibition additives.

Class of additives		Anti-oxygen inhibition effectiveness[a]	Typical characteristics					
			Storage stability	Odor	Toxicity	State of matter	Commercial availability	Other comments
Hydrogen donors	Amines	+	Good	Ammonia-like	Irritant	Liquid/solid	Yes	Yellowing; acrylated amines preferred
	Thiols	++	Poor[b]	Bad	Irritant	Liquid	Yes	Odorless oligomeric thiols available
	Hydrogen phosphites	+	Probably poor	Phenolic	Irritant	Liquid	Limited	Moisture sensitive
	Silanes	+	Poor	Faint	Irritant	Liquid	Limited	Moisture sensitive
	Stannanes	+++	Decomposes immediately	Stench	Toxic	Liquid	Limited	Moisture sensitive
	Benzaldehydes	−	Good	Almond-like	Irritant, toxic	Liquid	Yes	
N-vinyl amides		+	Good	Faint	Toxic	Liquid	Yes	Water uptake
Reducing agents	Aromatic phosphines	+++	Poor	Faint	Irritant, toxic	Solid	Yes	Oxidation sensitive
	Aliphatic phosphines	+	Poor	Faint	Corrosive, irritant	Solid	Yes	Oxidation sensitive
	Phosphites	+++	Poor[c]	Phenolic[c]	Irritant	Liquid	Yes	Oxidation sensitive
	Sulphites	+	Probably poor	Pungent	Irritant	Liquid	Yes	Oxidation sensitive
	Borane–amine complexes	+	Good	Ammonia-like	Toxic	Solid	Limited	
Sensitizers		++	Good	Odorless	Irritant	Solid	Yes	No photobleaching
Molecular inerting	NPG and its derivatives	−	Fair	Faint	Non-toxic	Solid	Limited	
	Oxime esters	+	Good	Odorless	Irritant	Solid	Limited	
$^1O_2$ scavengers		+	Good	Odorless	Irritant, toxic	Solid	Limited	Photobleaching

[a] Where "+++" is excellent (>25%), "++" is good (15–25%), "+" is poor (5–14%), and "−" is negligible (<5%).
[b] Stability increased with radical inhibitor and phosphonic acid [38,39].
[c] Stability and odor issue improved by complexing with aldehydes [42].

($Me_2NH·BH_3$) with a Type I photoinitiator (BDMB) only. The effect was comparable to that of amines (38% DBC) but the used amount of $Me_2NH·BH_3$ was halved compared to MDEA. Surprisingly, in the presence of ITX (0.1 eq.) the increase in DBC was negligible. Under these conditions the effect of boranes is questionable and may not justify its use in light of issues such as cost, stability, and solubility.

3.4. Molecular inerting

Some radical photoinitiators undergo decomposition to provide initiating radicals and a molecule of CO_2. While the principal advantage of gas generation may be entropic, this gas has a potential to suppress oxygen inhibition by replacing

oxygen in the formulation. As representatives of this class of molecules, *N*-phenyl glycine (NPG), *N*-methyl-*N*-phenyl glycine (NMNPG), and phenylthioacetic acid (PTAA) were chosen. These compounds are used in combination with a photosensitizer such as ITX and decompose according to the following scheme (Scheme 5a). *O*-benzoyloxime benzaldehyde (POE) and 1-phenyl-1,2-propanedione-2-(*O*-ethoxycarboxy)oxime (PDO) are representatives of oxime esters – another class of CO_2 producers. Oxime esters can be sensitized by ITX and cleave at the N—O bond. The formed benzoyloxy radical tends to decarboxylate (Scheme 5b).

NPG, NMNPG and PTAA showed all negligible improvements in DBC after curing. Although the formation of CO_2 has been proven [35], the amount of CO_2 may not be sufficient to exclude oxygen from the films during the curing process. ITX, which is ideally used in equimolar ratio to these compounds, cannot be used at higher concentration due to its distinct non-photobleachable yellow color. By comparison, oxime esters (POE, PDO) seem to be a promising strategy at first, with improvement in DBC from 42 to 49% at low additive content (0.3 eq.). One has to keep in mind that besides being CO_2 producers, POE and PDO are also photoinitiators absorbing at 365 nm similarly to BDMB. It is thus difficult to quantify whether improvement in DBC is due to molecular inerting or due to the presence of additional initiating radicals. By comparison, addition of 0.3 eq. BDMB to base formulation with 0.1 eq. ITX improves curing to 55% DBC.

3.5. Singlet oxygen scavengers

In contrast to ground state triplet oxygen ($^3O_2$), singlet oxygen ($^1O_2$) does not react with carbon-centered radicals during the polymerization. $^1O_2$ can however react with unsaturated hydrocarbons in a variety of manners. Due to the short life-time of $^1O_2$, it is essential to trap it before can relax back to $^3O_2$ or react with other the components of the formulation. This is accomplished by using singlet oxygen scavengers, which undergo [4 + 2] cycloaddition reactions (Scheme 6). $^1O_2$ can be generated by a suitable photosensitizer, which after excitation transfers energy to $^3O_2$. ITX is chosen here as sensitizer since it absorbs well at the utilized LED frequencies.

In previous investigations, 2,5-diphenyl furan (DPF) gave very promising results in a formulation containing camphorquinone as the initiator reaching the same DBC in air as the formulation without DPF cured under nitrogen [14]. However, in this study the use of DPF without or with ITX did not increase double bond conversion.

The usage of 9,10-dibutyl anthracene (DBA) alone does not show any improvement in reducing oxygen inhibition. However, in combination with ITX, DBC in the final films was improved from 42% to 55%. Important to clear coat applications, DBA photobleaches upon curing and the photoproduct is a stable molecule. DBA showed good storage stability in the formulation with no significant decomposition within 30 days.

3.6. Overview

A plethora of anti-oxygen inhibition additives have been reported to date. We have attempted to reassess multiple strategies by testing representative additives under comparable conditions and summarize these results in Table 1. This summary provides guidelines to the formulator by comparing different additives in terms of their effectiveness and related issues such as storage stability, odor, toxicity, miscibility, commercial availability and others.

4. Conclusions

To provide a suitable alternative to nitrogen inerting, a variety of additives for mitigating oxygen inhibition were evaluated in acrylate formulation under LED curing. While improvements were made, no ultimate solution to this problem has yet been found. Reducing agents are the most effective additives in improving final cure, however formulations are in almost all cases not storage stable. Triphenyl phosphine and tris(tridecyl) phosphite enhanced the curing the most. Aromatic and hybrid aromatic/aliphatic phosphites were found to slightly less effective with similar storage stability problems. Hydrogen donors were found to improve cure up to a certain extent but due to different limitations only amines, borane-amine complexes and thiols seem applicable industrially. *N*-vinyl amides are suitable for applications where increased hydrophilicity and reduction in viscosity can be accepted.

Since LEDs were used for these studies, the effect of different wavelengths could also be investigated. Dual wavelength (365/400 nm) curing was found to provide some advantages. In which case, a sensitizer absorbing at a different wavelength from the photoinitiator may work in combination with another additive. The use of singlet oxygen scavengers is also a promising approach but has not attracted industry's attention so far. Of the CO_2 producing species, only the oxime esters provided improvement. The use of multiple additives may be promising, although a proper systematic investigation is outside the scope of the present work.

Appendix A. Supplementary data

Supplementary data associated with this article can be found, in the online version, at http://dx.doi.org/10.1016/j.porgcoat.2014.06.005.

References

[1] P. Collins, Woodcoatings – technology and market developments, in: PRA's 8th International Woodcoatings Congress, Amsterdam, NL, 2012.
[2] UVLED energy efficient curing. http://www.fp7-uvled.eu/ (accessed on 21.11.13).
[3] S.C. Ligon, B. Husár, H. Wutzel, R. Holman, R. Liska, Chem. Rev. 114 (2014) 557–589.
[4] L. Gou, B. Opheim, A.B. Scranton, Methods to overcome oxygen inhibition in free radical photopolymerizations, in: J.P. Fouassier (Ed.), Photochemistry and UV Curing: New Trends, Research Signpost, Trivandrum, 2006, pp. 301–310.
[5] C. Hoyle, M. Cole, W. Kuang, S. Jonsson, C. Nason, T. Ishijima, R. Kess, K. Viswanathan, T.Y. Lee, R. Ng, R. Miller, RadTech Rep. 16 (2002) 47–56.
[6] K. Dietliker, A Compilation of Photoinitiators Commercially Available for UV Today, SITA, Edinburgh, 2002.
[7] D. Harbourne, An update on the current market situation for UV/EB curing and an insight into the development of new markets for UV/EB processing, in: RadTech Asia, Shanghai, CN, 2013.
[8] K. Studer, C. Decker, E. Beck, R. Schwalm, Prog. Org. Coat. 48 (2003) 92–100.
[9] K. Studer, C. Decker, E. Beck, R. Schwalm, Prog. Org. Coat. 48 (2003) 101–111.
[10] R. Müller, UV-cross linking under oxygen-reduced conditions, in: RadTech Europe 01, Basel, CH, 2001, pp. 149–152.
[11] T. Henke, UV inert technology of today and development for the future, in: RadTech Europe 01, Basel, CH, 2001, pp. 145–148.
[12] D.A. Bolon, K.K. Webb, J. Appl. Polym. Sci. 22 (1978) 2543–2551.
[13] C. Decker, Polym. Int. 45 (1998) 133–141.

[14] M. Höfer, N. Moszner, R. Liska, J. Polym. Sci. A: Polym. Chem. 46 (2008) 6916–6927.
[15] C. Decker, Die Makromol. Chem. 180 (1979) 2027–2030.
[16] L. Gou, B. Opheim, C.N. Coretsopoulos, A.B. Scranton, Chem. Eng. Commun. 193 (2006) 620–627.
[17] S. Jauk, R. Liska, J. Macromol. Sci. A: Pure Appl. Chem. 45 (2008) 804–810.
[18] G.L. Collins, J.R. Costanza, J. Coat. Technol. Res. 51 (1979) 57–63.
[19] N.B. Cramer, C.N. Bowman, J. Polym. Sci. A: Polym. Chem. 39 (2001) 3311–3319.
[20] T.Y. Lee, C.A. Guymon, E.S. Jönsson, C.E. Hoyle, Polymer 45 (2004) 6155–6162.
[21] J. Lalevée, M.A. Tehfe, F. Morlet-Savary, B. Graff, X. Allonas, J.P. Fouassier, Prog. Org. Coat. 70 (2011) 83–90.
[22] M. El-Roz, J. Lalevée, X. Allonas, J.P. Fouassier, Macromolecules 42 (2009) 8725–8732.
[23] B. Xiao, Y. Zhou, S. Li, M. Luo, X. Wang, P. Zhao, Radiat. Phys. Chem. 57 (2000) 421–424.
[24] J. Le Guern, H. Farge, X. Allonas, J. Lalevée, J.P. Fouassier, Method for free radical polymerisation and radiation polymerizable composition obtained by said method (assigned to A et A Mader, Centre National de la Recherche Scientifique, Université de Haute Alsace) WO 2009/071844A1 (2009).
[25] C. Belon, X. Allonas, C. Croutxé-Barghorn, J. Lalevée, J. Polym. Sci. A: Polym. Chem. 48 (2010) 2462–2469.
[26] W. Schmitt, R. Purrmann, P. Jochum, Photopolymerizable compositions based on acrylic or methacrylic acid esters containing organic phosphites (assigned to ESPE Fabrik Pharmazeutischer Praeparate GmbH) US 4,189,365A (1980).
[27] A.V. Fedorov, A.A. Ermoshkin, A. Mejiritski, D.C. Neckers, Macromolecules 40 (2007) 3554–3560.
[28] F. Courtecuisse, A. Belbakra, C. Croutxé-Barghorn, X. Allonas, C. Dietlin, J. Polym. Sci. A: Polym. Chem. 49 (2011) 5169–5175.
[29] F. Morlet-Savary, F. Wieder, J.P. Fouassier, J. Chem. Soc. Faraday Trans. 93 (1997) 3931–3937.
[30] L. Feng, B.I. Suh, J. Appl. Polym. Sci. 112 (2009) 1565–1571.
[31] D. James, Unique characteristics of a dendritic polyether for radiation curing, in: PRA Radcure Coatings and Inks, Manchester, UK, 2002.
[32] C.W. Miller, C.E. Hoyle, S. Jönsson, C. Nason, T.Y. Lee, W.F. Kuang, K. Viswanathan, ACS Symp. Ser. 847 (2003) 2–14.
[33] F. Morel, C. Decker, S. Jönsson, S.C. Clark, C.E. Hoyle, Polymer 40 (1999) 2447–2454.
[34] C. Decker, D. Decker, J. Macromol. Sci. A: Pure Appl. Chem. 34 (1997) 605–625.
[35] S.-I. Murahashi, N. Komiya, H. Terai, T. Nakae, J. Am. Chem. Soc. 125 (2003) 15312–15313.
[36] C. Dworak, R. Liska, J. Polym. Sci. A: Polym. Chem. 48 (2010) 5865–5871.
[37] D. Leonhardt, D. Skinner, K. Kawamura, K. Ashikaga, D. Diehl, P.K. Swain, D. Harbourne, Advancements in UV LED technology and its impact on UV curing applications, in: RadTech Asia 2013, Shanghai, CN, 2013.
[38] P. Esfandiari, S.C. Ligon, J.J. Lagref, R. Frantz, Z. Cherkaoui, R. Liska, J. Polym. Sci. A: Polym. Chem. 51 (2013) 4261–4266.
[39] Z. Cherkaoui, P. Esfandiari, R. Frantz, J.-J. Lagref, R. Liska, Stable curable thiol-ene composition for lithography (assigned to Huntsman Advanced Materials GmbH) WO 2012/126695A1) (2012).
[40] A. Criqui, J. Lalevée, X. Allonas, J.P. Fouassier, J. Adv. Oxid. Technol. 12 (2009) 215–219.
[41] J.W. Chan, C.E. Hoyle, A.B. Lowe, M. Bowman, Macromolecules 43 (2010) 6381–6388.
[42] D. Shukla, Photocurable and photocured compositions (assigned to Eastman Kodak Company) WO 2012/112294A1 (2012).